

Effects of magnetic history on the ac magnetic susceptibility of granular $\text{YBa}_2\text{Cu}_3\text{O}_{7-8}$ superconductors in weak fields

Sang Young Lee

Department of Physics, Kon Kuk University, Seoul 133-701, Korea

Min Ah Suh,* Sang Min Bae,[†] and Sang Sam Choi

Applied Physics Laboratory, Korea Institute of Science and Technology, Seoul 136-791, Korea

In-Sang Yang

Department of Physics, Ewha Womans University, Seoul 120-750, Korea

(Received 17 November 1994; revised manuscript received 9 February 1995)

We investigate the ac susceptibility of both field-cooled and zero-field-cooled sintered $\text{YBa}_2\text{Cu}_3\text{O}_{7-8}$ granular thin slabs and powders in low magnetic fields. The ac susceptibility of the granular thin slabs appears to depend upon the magnetic history for dc fields larger than a certain value, H_{dc}^* , with the existence of the stronger diamagnetic signal (the in-phase part of the ac susceptibility) in the field-cooled case. Our results show that the difference in local flux distributions between the field-cooled case and the zero-field-cooled case exists even for a dc field as low as several Oe, a value much lower than the bulk lower critical field (H_{c1}). The upper limit of a homogeneous superconducting area determined from H_{dc}^* appears comparable to the average grain size in our granular thin slabs. The existence of H_{dc}^* is attributed to the superconducting glass behavior of granular $\text{YBa}_2\text{Cu}_3\text{O}_{7-8}$ with disorder in the intergranular Josephson junctions.

I. INTRODUCTION

Since the discovery of high- T_c superconductors (HTS), magnetic irreversibility in HTS, which has been observed in measurements of dc magnetization¹⁻³ and ac susceptibility,⁴⁻⁷ remains as one of the many controversial fields. In studies of the dc magnetization of field-cooled (FC) and zero-field-cooled (ZFC) granular La-Ba-Cu-O, Müller, Takashige, and Bednorz¹ reported a dc irreversibility line for HTS, a boundary between reversible and irreversible regions. According to them, the magnetization in their ZFC sample is larger than the FC one at temperatures below a certain temperature on the dc irreversibility line, which they ascribed to spin-glass-like behavior (henceforth, called superconducting glass behavior). Subsequent studies revealed that the superconducting glass (SG) behavior originates in the disorder of Josephson junctions inside the superconducting grains.^{3,8,9} Meanwhile, magnetic irreversibility in HTS has also been explained using a flux-creep model.¹⁰⁻¹² Yeshurun and Malozemoff² reported that the irreversibility could be explained using a flux-pinning picture and a simple scaling argument, which was extended by Tinkham in explaining the anomalous resistive broadening in HTS.¹³ Worthington, Gallagher, and Dinger,⁴ in their ac susceptibility measurements, also reported an ac irreversibility line in their measurements of frequency-dependent complex ac susceptibility (χ_{ac}) of single-crystal $\text{YBa}_2\text{Cu}_3\text{O}_{7-8}$ (YBCO). They explained that flux creep, which is significant in HTS due both to the relatively high operating temperature and to the low pinning energies, accounts for the observed ac irreversibility line. Up to date,

the two models (the SG model and the flux-creep model) are regarded as the key models in explaining the magnetic irreversibility in HTS, by many researchers.^{14,15} Recently, Ji, Rzchowski, and Tinkham¹⁶ reported an anomalous irreversibility in their measurements of surface resistance of granular YBCO. They observed that the surface resistance appeared larger in a ZFC sample than a FC one, in spite of the fact that more vortices presumably exist in the FC sample. They attributed this anomalous behavior to different local flux distributions originating from different magnetic history. Later, Perez, Obradors, and Fontcuberta¹⁷ also reported similar behavior in ac susceptibility of granular iron-doped YBCO (Y-Ba-Cu-Fe-O). In a dc field of 10 Oe, they observed that the absolute magnitude of the in-phase part of χ_{ac} (χ'_{ac}) of FC case (hereafter called $[\chi'_{ac}]_{FC}$) is larger than the corresponding value in the ZFC case (hereafter called $[\chi'_{ac}]_{ZFC}$) at temperatures below a certain value. However, the reason for different local flux distributions remains mostly unaddressed. Experiments by Ji, Rzchowski, and Tinkham were performed in a dc magnetic field of 120 Oe, which is believed to be higher than the lower critical field of YBCO at the liquid-nitrogen temperature. Meanwhile, experimental results of Perez, Obradors, and Fontcuberta revealed that the effect of local flux distributions could be observed in fields much lower than H_{c1} . However, since the experiment by Perez, Obradors, and Fontcuberta is on iron-doped YBCO having presumably a lower value of H_{c1} , the relation between the hysteretic behavior in ac susceptibility and the applied field remains to be resolved. In this paper, we report effects of magnetic history on the ac susceptibility of sintered YBCO su-

perconductors under weak magnetic fields. Dependences of the ac susceptibility on the temperature (T), the dc magnetic field, as well as on the sample morphology are investigated for granular YBCO samples. Analyses of our experimental data based on the SG model follow in order to address possible reasons for different local flux distributions between field-cooled and zero-field-cooled cases and the hysteretic ac susceptibility in granular YBCO.

II. EXPERIMENTAL

Granular YBCO samples were prepared both in thin slab and in powder forms from sintered bulk YBCO. Three different sintered YBCO bulk samples, bulk *A*, *B*, and *C*, with different grain sizes were used throughout the experiments. Bulk *A* was made using the conventional solid-state reaction process,¹⁸ and bulks *B* and *C* are prepared by sintering at 930°C for 12 h in O₂ environment followed by annealing at 500°C for 10 h in argon-oxygen gas mixtures. Two thin slab samples, samples *A1* and *A2*, were prepared from bulk *A* with the dimensions of 2×4×0.2 mm³ and 3×4×0.2 mm³, respectively. Different thin slab samples, samples *B* and *C*, prepared from bulks *B* and *C*, appeared to be 3×4×0.2 mm³ and 3×5×0.2 mm³ in size, respectively. The grain size in samples *A1* (and *A2*) is about 1–2 μm in length, and about 3–6 μm in samples *B* and *C*. The YBa₂Cu₃O_{7-δ} powder sample (sample AP) was prepared by pulverizing bulk *A* and collecting the grains using a 25 mesh sieve. Figures 1(a)–1(c) show the scanning electron microscope (SEM) pictures of samples *A1*, *B*, and *C*, respectively. A commercial ac susceptometer (Model 8000 from Lakeshore Cryogenics with model 5209 Lock-in amplifier from EG&G) employing a mutual inductance method was used for taking data in fields of $H_{dc}=0-10$ Oe and $H_{ac}=0.05-1.0$ Oe, and at temperatures between 57 and 95 K. To reduce demagnetization effects, thin slab samples were located in a teflon cell with the direction of the applied fields parallel to the long axes of the samples. Sample AP was first loosely packed into a glass cylinder, before being placed in the teflon cell. Ac susceptibility data were taken with increasing temperature both for FC and ZFC cases. Samples were cooled in the ambient earth field in the ZFC case, while a dc field was applied during cooling in the FC case. To eliminate any effect of remanent magnetic moment, the temperature was raised to about 100 K after taking each set of data for a combination of a dc field and an ac field. The susceptibility sensitivity was about 1/10 000–2/10 000 (SI unit) in volume susceptibility ($\chi_{ac}=M/H$ in SI unit, dimensionless) during measurements. A data point was collected every 4 min including 2 min for temperature stabilization at a temperature interval of 0.1 K. The temperature was stable within 0.02 K and the frequency of the applied ac field was set to 111.1 Hz throughout our experiments. Our experimental data appeared reproducible within the sensitivity of our measurements when we checked it each time before completing a series of experiments with a sample. The demagnetization factor is assumed to be zero.

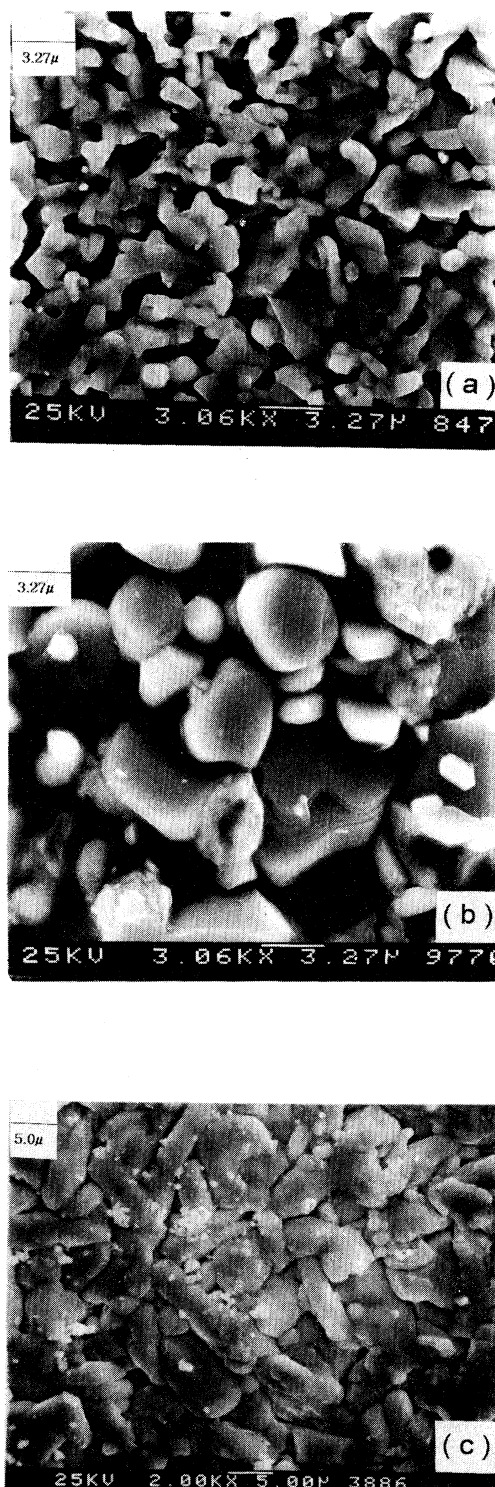


FIG. 1. (a) An SEM picture of sample *A1* (bulk *A*). Most grains are about 1–2 μm in size. (b) An SEM picture of sample *B* (bulk *B*). Most grains appear 3–6 μm in size, larger than the average grain size in sample *A1* (bulk *A*). (c) An SEM picture of sample *C* (bulk *C*). Most grains appear 3–6 μm in size, comparable to the grain size in sample *B* (bulk *B*) and larger than the average grain size in sample *A1* (bulk *A*).

III. RESULTS AND DISCUSSIONS

In Fig. 2(a), we show the ac field dependence of χ_{ac} vs T curves measured in ambient earth field for sample *A1*. A strong ac field dependence of both χ'_{ac} and the out-of-phase part of χ_{ac} (χ''_{ac}) is seen in the figure, with T_p , the temperature of a peak in χ''_{ac} , shifted to a lower value with increase of H_{ac} . Similar results have previously been reported by many researchers, for which different models such as the flux-creep model/critical-state model^{19–21} and the SG model^{22–24} have been proposed. Figure 2(b) shows ZFC data for sample *A1* in $H_{dc}=5$ and 9 Oe and $H_{ac}=0.1$ and 1 Oe. We note in the figure suppression of the in-phase signal χ'_{ac} and a shift of T_p in χ''_{ac} to a lower value for higher H_{dc} , which can be attributed to the weaker intergranular couplings in the specimen by application of a higher dc field. In Fig. 3(a), both ZFC and FC data are displayed for sample *A1* in $H_{dc}=5$ Oe and $H_{ac}=0.05, 0.5, \text{ and } 1$ Oe, where data appear reversible for each set of H_{ac} and H_{dc} between FC and ZFC cases.

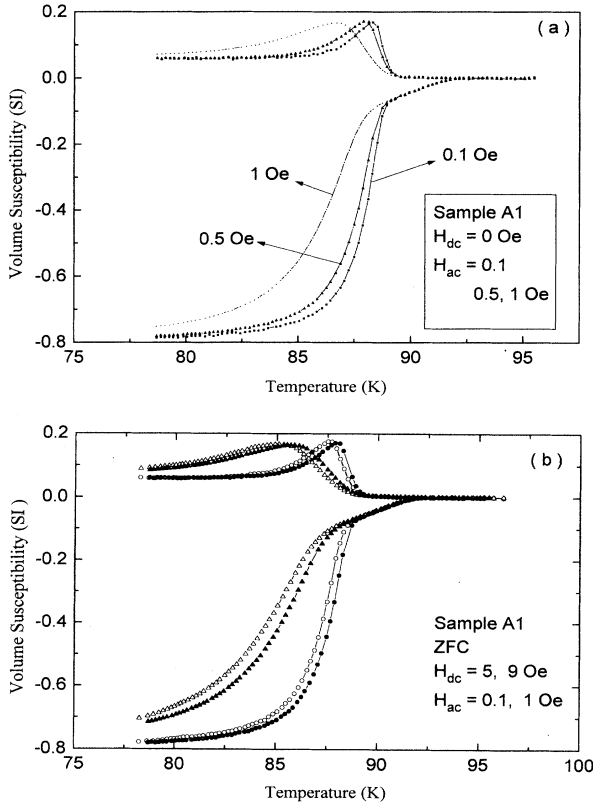


FIG. 2. (a) Ac field dependence of the χ_{ac} (volume susceptibility) vs T curves for $H_{ac}=0.1, 0.5, 1$ Oe measured in ambient earth field for sample *A1*. The absolute magnitudes of χ'_{ac} are saturated to a value less than 1 near 77 K due to errors in estimation of the sample volume. (b) Dc field dependence of the χ_{ac} (volume susceptibility) vs T curves for $H_{dc}=5$ (filled circle and triangle) and $H_{dc}=9$ Oe (open circle and triangle): the filled circle is for $H_{ac}=0.1$ Oe, $H_{dc}=5$ Oe, the open circle for $H_{ac}=0.1$ Oe, $H_{dc}=9$ Oe, the filled triangle for $H_{ac}=1$ Oe, $H_{dc}=5$ Oe, and the open triangle for $H_{ac}=1$ Oe and $H_{dc}=9$ Oe.

In fact, χ_{ac} vs T data appeared reversible for dc fields less than 5 Oe regardless of the change in H_{ac} (small differences seen at temperatures below 80 K may be due to temperature fluctuations at the initial stage of measurements, which disappeared in a measurement down to 57 K). Meanwhile, when H_{dc} is as high as 8 Oe, χ_{ac} vs T data show different behavior for sample *A1*. Figure 3(b) shows ZFC and FC data for sample *A1* in fields of $H_{dc}=8$ Oe and $H_{ac}=0.05, 0.5, \text{ and } 1$ Oe at temperatures above 57 K. In the figure, χ_{ac} vs T data appear reversible at temperatures above T_1 and below T_2 . However, the absolute magnitude of χ'_{ac} for the FC sample ($[\chi'_{ac}]_{FC}$) appears larger than the value for the ZFC sample ($[\chi'_{ac}]_{ZFC}$) at temperatures between T_1 and T_2 for all ac fields, showing irreversibility in the temperature region. Due to accidental exposure of sample *A1* to moisture, a more systematic study on the ac susceptibility of bulk *A* for $H_{dc} \geq 6$ Oe was performed with sample *A2* (another sample prepared from bulk *A*) in dc fields of 6, 7, 8, 9, and 10 Oe. Figure 3(c) displays χ_{ac} vs T plots for sample *A2* in fields of $H_{dc}=6$ and 10 Oe and $H_{ac}=0.5$ Oe. Here the data appeared irreversible between T_1 and T_2 with the respective value of T_1 about 89.1 K for $H_{dc}=6$ Oe and 88.5 K for $H_{dc}=10$ Oe. For temperatures above T_1 and below T_2 , χ_{ac} appears reversible. We observe similar behavior in the data for samples *B* and *C*. In Fig. 4(a), the data for $H_{dc}=2, 3, \text{ and } 10$ Oe are plotted for sample *B*, where we see irreversible χ_{ac} vs T for $H_{dc} \geq 3$ Oe. Figures 4(b)–4(d) show χ_{ac} vs T data for sample *C*, where the data appear reversible for $H_{dc}=1$ Oe and irreversible for $H_{dc} \geq 2$ Oe. Our results, being in qualitative agreement with the previous report by Perez, Obradors, and Fontcuberta,¹⁷ contain experimental findings. First of all, the value of T_p^* , the temperature giving maximum in $\delta\chi'_{ac}$ is close to T_p , with $\delta\chi'_{ac}$ denoting the differences between $[\chi'_{ac}]_{ZFC}$ and $[\chi'_{ac}]_{FC}$. This result, as displayed in Figs. 5(a) and 5(b) for samples *A2* and *C*, respectively, seems to be consistent with the earlier suggestions by Clem²⁵ and Gershkenbein, Vinokur, and Fehrenbacher.²⁶ They suggest that T_p in χ''_{ac} corresponds to the temperature where H_{ac} fully penetrates the sample. In this regard, effects of different local flux distributions on χ_{ac} would be maximum at T_p , yielding maximum difference in χ'_{ac} at this temperature. As the penetration depth gets smaller at a lower temperature than T_p , the difference in χ_{ac} becomes smaller and unobservable at T_2 [see Figs. 3(b) and 3(c) for sample *A2*, and Figs. 4(a)–4(c) for sample *B* and *C*, respectively]. We also see in Figs. 4(a) and 4(b) that the χ_{ac} vs T data appear slightly shifted to lower temperature in the ZFC case compared to the one in the FC case, signalling an increase of effective flux density in the intergranular regions in the ZFC case compared to the FC case. We note here that this is not clearly observed for sample *A2* due to errors in experimental data [Fig. 5(a)]. However, the difference between $[T_p]_{FC}$ and $[T_p]_{ZFC}$ is seen more clearly for sample *C*. In Fig. 5(b), the values of T_p in ZFC sample ($[T_p]_{ZFC}$) appear slightly lower than the values in the FC case ($[T_p]_{FC}$) for all H_{dc} fields.

Secondly, $\delta\chi'_{ac}$ increases as the magnitude of H_{dc} gets

higher for $H_{dc} \geq H_{dc}^*$ ($H_{dc}^* \approx 6, 3,$ and 2 Oe for samples $A2, B,$ and $C,$ respectively), indicating that the difference in the effective flux density in the intergranular region increases for higher H_{dc} between FC and ZFC cases. Thirdly, χ_{ac} vs T data appear reversible for $H_{dc} \leq H_{dc}^*$, with the magnitude of H_{dc}^* different among samples $A1$ (or $A2$), $B,$ and $C,$ i.e., χ_{ac} vs T being reversible for $H_{dc} \leq 5$ Oe in sample $A1$ (or presumably in sample $A2$) while being so for $H_{dc} \leq 2$ Oe in sample B and $H_{dc} \leq 1$ Oe in sample C . Within our contexts, reversibility in χ_{ac} should mean no trapped flux in the individual $\text{YBa}_2\text{Cu}_3\text{O}_{7-\delta}$ grain during the field-cooling process, which results in the same flux distributions in the intergranular region for the FC and ZFC cases. Several questions are to be raised at this moment. (1) Is the irreversibility in the χ_{ac} vs T data due to intergranular properties and/or intragranular properties of granular samples? (2) How can we explain the existence of H_{dc}^* ? (3) Why is the

magnitude of H_{dc}^* different among samples $A1$ (or $A2$), B and C ? To find a clue for the first question, we experimented with YBCO powder sample AP prepared from bulk $A,$ where the number of intergranular Josephson junctions (or called grain-boundary junctions) among superconducting YBCO grains are assumed to be much smaller than in sample $A1$ (or $A2$). Figure 6 shows the ac susceptibility data with $H_{ac} = 0.5$ Oe and $H_{dc} = 12$ Oe for sample AP, where reversibility in χ_{ac} vs T is noted. This is in contrast with the data for samples $A1$ and $A2,$ implying that the magnetic history-dependent irreversibility in χ_{ac} vs T for sintered polycrystalline YBCO be attributed to the existence of the intergranular Josephson junctions. As previously reported by other researchers,^{27,28} intergranular peaks in χ_{ac}'' are not observable in the powder sample AP. For the second question, we propose the following. Due to the extremely short coherence lengths in HTS, we can think of each YBCO grain in the

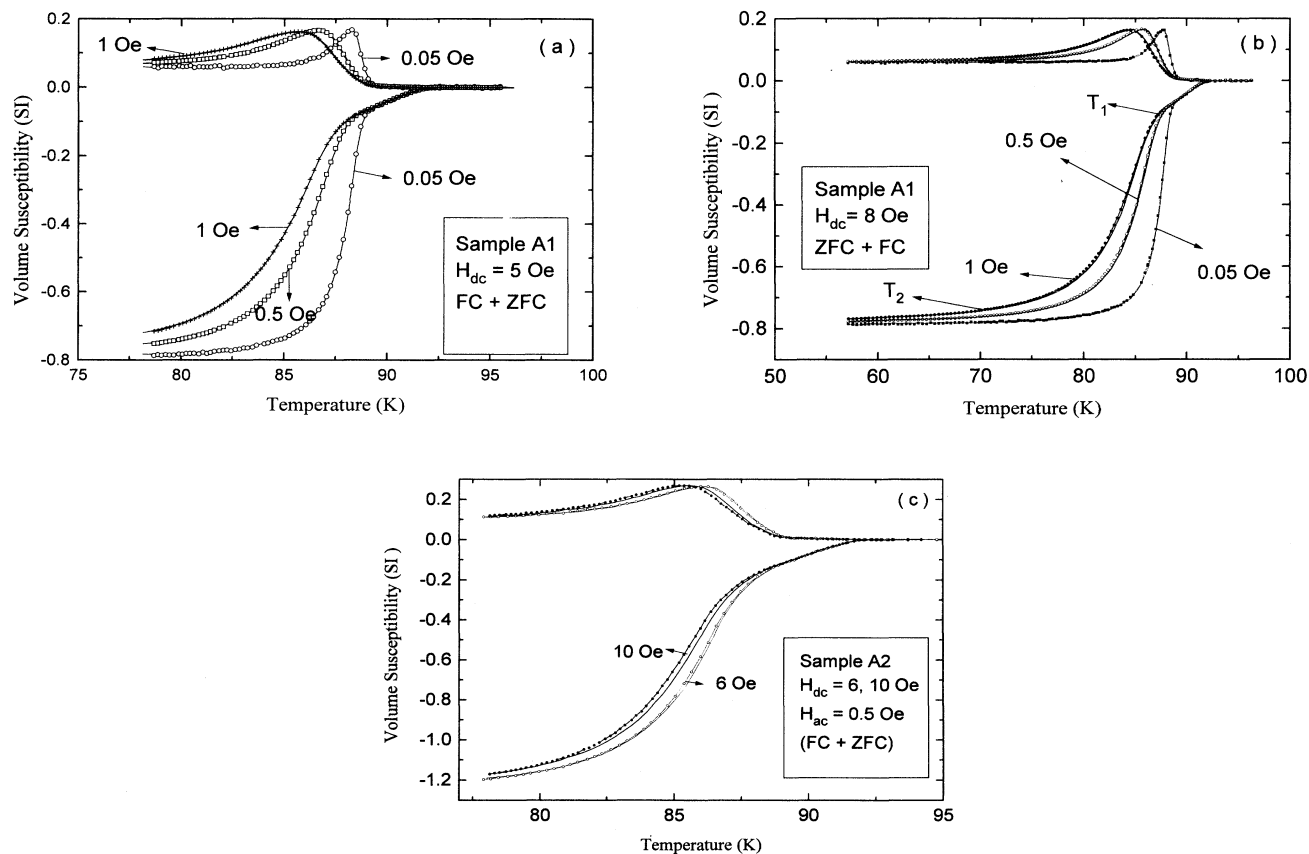


FIG. 3. (a) χ_{ac} vs T data for sample $A1$ in fields of $H_{dc} = 5$ Oe and $H_{ac} = 0.05, 0.5,$ and 1 Oe for ZFC (symbols) and FC (solid lines) cases. No difference is seen down to 80 K between the two cases regardless of increase of H_{ac} by 20 times. Small differences below 80 K are attributed to temperature fluctuations at the initial stage of measurements. (b) χ_{ac} vs T data for sample $A1$ in fields of $H_{dc} = 8$ Oe and $H_{ac} = 0.05, 0.5,$ and 1 Oe for ZFC (line + symbol) and FC (solid line) cases. χ_{ac} vs T data is irreversible at temperatures between T_1 and T_2 and reversible at temperatures less than T_2 and higher than T_1 (note that the data for $H_{ac} = 0.05$ Oe also showed irreversibility, which look reversible due to the steepness of the χ_{ac}' vs T curves near T_1). (c) χ_{ac} vs T plots for sample $A2$ in fields of $H_{dc} = 6$ and 10 Oe and $H_{ac} = 0.5$ Oe for ZFC (line + symbol) and FC (solid line) cases. Irreversibility in χ_{ac} vs T is clearly seen with larger difference for $H_{dc} = 10$ Oe. Here the absolute magnitudes of χ_{ac}' are saturated to a value larger than 1 near 77 K since demagnetization factor is set to zero. Another crossover at temperatures below T_2 is attributed to temperature fluctuations at the initial stage of measurements.

samples as a three-dimensional Josephson array with intragranular Josephson couplings. In this regard, a YBCO thin-slab sample can be regarded as a Josephson array with intragranular Josephson couplings inside the grains and intergranular Josephson couplings among the grains. In general, a Hamiltonian of a system with coupled superconducting elements is given by

$$\mathbf{H} = - \sum J_{ij} \cos(\phi_i - \phi_j - A_{ij}) \quad (1)$$

with J_{ij} being the temperature-dependent Josephson coupling energy between the superconducting elements i and j , ϕ_i and ϕ_j the phase of the elements i and j , respectively. The phase factor A_{ij} is given by

$$A_{ij} = \frac{2\pi}{\Phi_0} \int_i^j \mathbf{A} \cdot d\mathbf{l} \quad (2)$$

with \mathbf{A} denoting the vector potential and $d\mathbf{l}$ the line vector connecting the superconducting elements i and j , and

Φ_0 an elementary flux quantum. Here we note that the elements i and j in Eqs. (1) and (2) are not necessarily the visual grains in our samples and that, based on previous experimental reports, the magnitude of intragranular J_{ij} (J_{ij}^{intra}) is 10^3 – 10^4 higher than the intergranular J_{ij} (J_{ij}^{inter}). Both J_{ij}^{intra} and J_{ij}^{inter} are expected to have the same temperature dependence of $(1 - T/T_c)^2$ due to the short coherence lengths of HTS.⁸ According to Ebner and Stroud,²⁹ superconducting clusters with disordered Josephson junctions show magnetic irreversibility between the FC and ZFC cases due to the existence of frustration, which makes a cluster hop from one configuration to another in order to stay in the ground state. Their numerical calculations reveal that the first phase slip in A_{ij} occurs at fields near H^* , with H^* determined by $H^* \cdot (2S) = \Phi_0$. Here S denotes the projected area of a homogeneous superconducting cluster perpendicular to the magnetic field. In our picture, we note that a whole thin-slab sample contains both intragranular

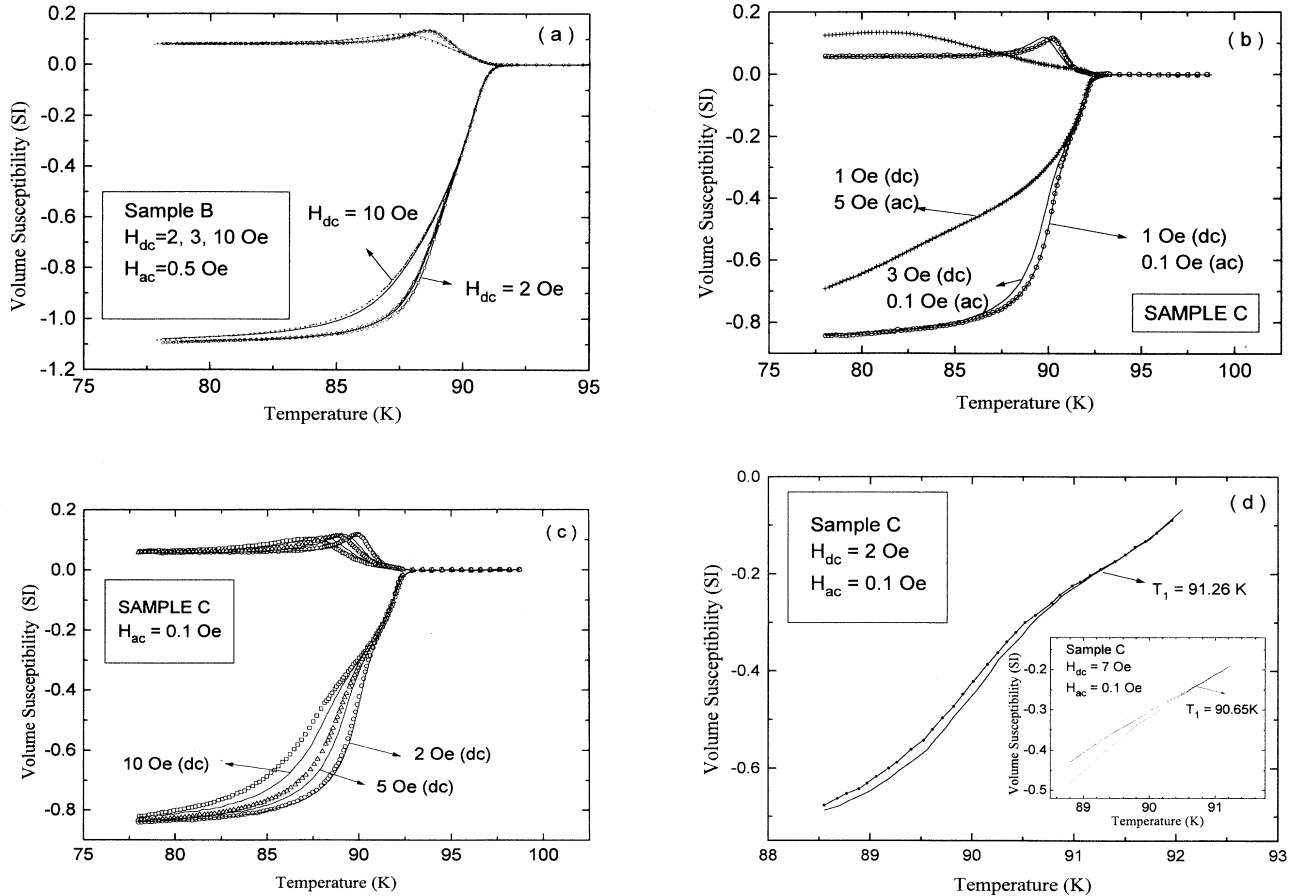


FIG. 4. (a) χ_{ac} vs T curves both for ZFC (symbol+line) and FC (solid line) sample *B* in fields of $H_{dc} = 2, 3,$ and 10 Oe and $H_{ac} = 0.5$ Oe. The data appear reversible for $H_{dc} = 2$ Oe, while being irreversible for H_{dc} larger than 3 Oe. (b) χ_{ac} vs T curves both for ZFC (symbol) and FC (solid line) sample *C* in fields of $H_{dc} = 1$ Oe and $H_{ac} = 0.1$ and 5 Oe. The data appear reversible for $H_{dc} = 1$ Oe irrespective of an increase in H_{ac} by 50 times. The data for $H_{dc} = 3$ Oe (solid line) are presented here for reference. (c) χ_{ac} vs T curves both for ZFC (symbol) and FC (solid line) sample *C* in fields of $H_{dc} = 2, 5,$ and 10 Oe and $H_{ac} = 0.1$ Oe. The data appear irreversible for all dc fields larger than 2 Oe. (d) χ_{ac} vs T curves both for ZFC (symbol+line) and FC (solid lines) sample *C* in fields of $H_{dc} = 2$ Oe and $H_{ac} = 0.1$ Oe near T_1 . Inset shows χ_{ac} vs T data for $H_{dc} = 7$ Oe and $H_{ac} = 0.1$ Oe.

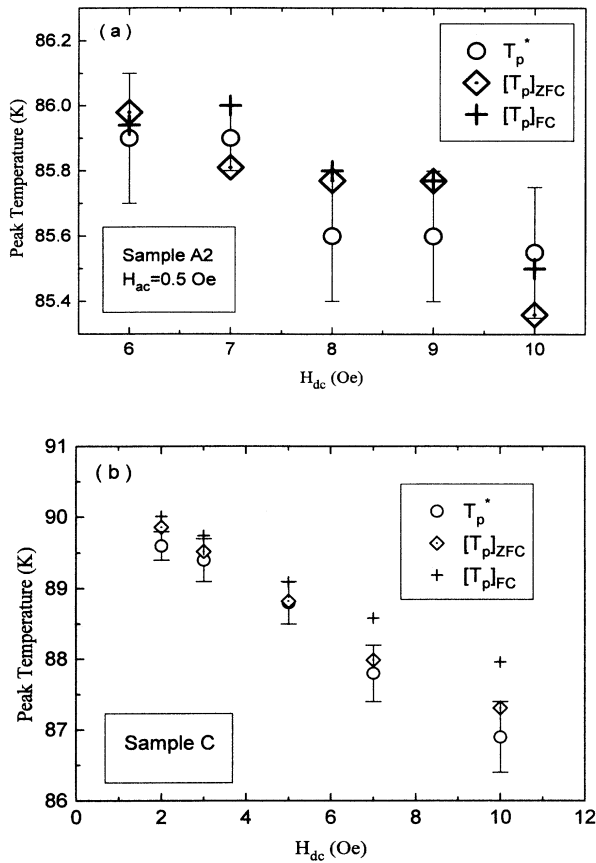


FIG. 5. (a) Dc field dependence of the temperatures giving peaks in χ''_{ac} in ZFC case ($[T_p]_{ZFC}$), in FC case ($[T_p]_{FC}$), and in $\delta\chi''_{ac}(T_p^*)$ for sample A2. The error bars are drawn for T_p^* , and the vertical sizes of the other symbols represent the error sizes. (b) DC field dependence of the temperatures giving peaks in χ''_{ac} in ZFC case ($[T_p]_{ZFC}$), in FC case ($[T_p]_{FC}$), and in $\delta\chi''_{ac}(T_p^*)$ for sample C. The error bars are drawn for T_p^* , and the vertical sizes of the other symbols represent the error sizes.

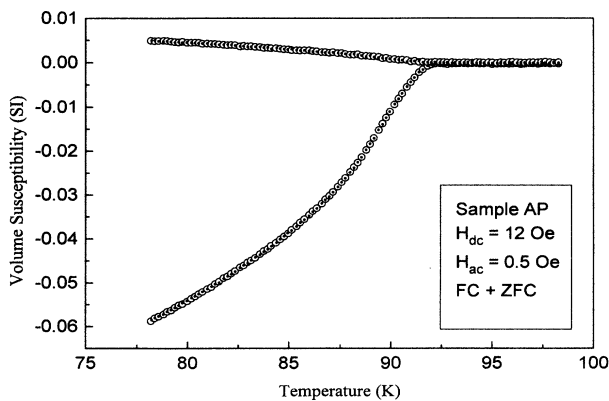


FIG. 6. The ac susceptibility data of powder sample AP for ZFC case (open symbol) and FC case (filled dot) in fields of $H_{dc} = 12$ Oe and $H_{ac} = 0.5$ Oe. Reversibility in χ_{ac} vs T curves are seen between the two cases.

Josephson junctions and intergranular Josephson junctions. Since J_{ij}^{intra} is much larger than J_{ij}^{inter} , each YBCO grain can be thought of as a homogeneous superconducting cluster with most of disorders attributed to intergranular Josephson junctions. Taking the measured value of H_{dc}^* for H^* , we get S about $2 \mu\text{m}^2$ for sample A1 (or A2). This gives $d = 1.5 \mu\text{m}$, with the value of d , the dimension of a square having the area S , which is comparable to the grain size of $1-2 \mu\text{m}$ for sample A1 (or A2) [see Fig. 1(a)]. Within this context, we expect smaller H_{dc}^* in sample B compared to sample A1 (or A2), for sample B has larger grain size than sample A1 (or A2). Taking the measured value of H_{dc}^* for H^* with the respective values of 2–3 Oe and 1–2 Oe for samples B and C, we get S less than $5 \mu\text{m}^2$ (i.e., $d < 2.2 \mu\text{m}$) for sample B and $10 \mu\text{m}^2$ (i.e., $d < 3.2 \mu\text{m}$) for sample C. These observations are consistent with the fact that the average grain size in samples B and C appear larger than that in sample A1 (or A2) [see Figs. 1(a)–1(c)], giving a possible answer for the third question. As the dc field increases, the effective homogeneous superconducting area S seems to be smaller with the reduced intergranular Josephson coupling strength. As a result, we expect lower T_1 for higher dc field (note that T_1 is the temperature above which χ_{ac} appeared reversible). In Figs. 7(a) and 7(b), we

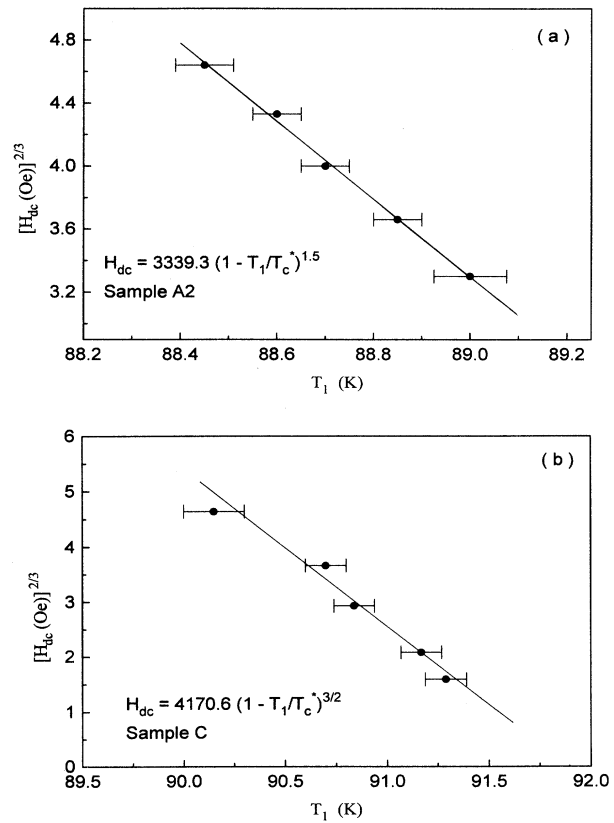


FIG. 7. (a) Variations of T_1 on the change of H_{dc} for sample A2. The solid line is a fit to an equation, $H_{dc} \text{ (Oe)} = 3339.3 (1 - T_1/T_c^*)^{1.5}$ with the fitted value of $T_c^* \approx 90.4$ K. (b) Variations of T_1 on the change of H_{dc} for sample C. The solid line is a fit to an equation, $H_{dc} \text{ (Oe)} = 4170.6 (1 - T_1/T_c^*)^{3/2}$ with the fitted value of $T_c^* \approx 91.9$ K.

show the dependence of T_1 on H_{dc} , for samples A2 and C. Within our experimental errors, the relations between H_{dc} and T_1 appear to be fitted to the same equation describing the H vs T irreversibility line in a glassy system.³⁰ We may raise another question at this moment. Is there any possibility of H_{dc}^* being related to H_{c1}^3 , the lower critical field of single crystal $\text{YBa}_2\text{Cu}_3\text{O}_{7-\delta}$? Cronmeyer and Holtzberg's report on dc susceptibility of some YBCO single crystals reveal the same value for the FC and ZFC cases for dc fields less than about 10 G, implying the possibility of small H_{c1} .³¹ To clarify this point, we compared two different sets of ac susceptibility data; one for sample A2 field-cooled down to 57 K, a value well below the liquid-nitrogen temperature, and the other for the same sample field-cooled to 85 K, the temperature giving almost maximum $\delta\chi'_{ac}$, in a dc field of 10 Oe. If the applied dc field of 10 Oe is small enough to be completely expelled from the individual YBCO grain at 57 K, we are likely to see a difference between the data for the field-cooled sample to 57 and 85 K because the sample field-cooled to 57 K is virtually in the same situation with the one zero-field-cooled to the same temperature. It turned out that the two sets of data appeared the same with each other for $T \geq 85$ K within the sensitivity of our apparatus (1/10 000–2/10 000 SI unit), exempting the relevance of nonzero $\delta\chi'_{ac}$ to H_{c1} .

Our observations are interesting in that they provide evidence for the role of SG behavior in ac susceptibility of bulk granular YBCO as well as in different local flux distributions between the zero-field-cooled case and the field-cooled case. The similarity between the magnitude of S and the average grain size indicates that our granular samples can be treated as weakly linked superconducting clusters with disorder in the intergranular Josephson junctions. This also provides a correlative result to the glassy behavior which has been observed in single-crystal HTS under strong magnetic fields of several Tesla, where disorder in Josephson junctions are attribut-

ed to the extremely small coherence length of HTS materials.³² For instance, Müller and co-workers^{1,8} and Blazey *et al.*⁹ reported values of S much smaller than the average grain size, while Kwak *et al.*³³ and Tiernan and Hallock³⁴ reported values of S comparable to the average grain size. The value of S much smaller than the average grain size is related to the glassy behavior originated from disorder in the intragranular Josephson junctions, while the value of S comparable to the grain size is related to the glassy behavior due to disorder in the intergranular Josephson junctions. Our results are also in agreement with a recent report by Jin *et al.*, who explained their ac susceptibility data of melt-textured YBCO using the vortex-glass model.³⁵

In summary, we report the ac susceptibility of both field-cooled and zero-field-cooled sintered $\text{YBa}_2\text{Cu}_3\text{O}_{7-\delta}$ samples both in thin slab and in powder forms. It appears that the hysteretic ac susceptibility between field-cooled and zero-field-cooled cases depends on the magnitude of the applied dc fields, with irreversibility observed for dc fields larger than H_{dc}^* . Its magnitude turned out much lower than the bulk lower critical field. The hysteretic ac susceptibility data are compatible with the superconducting glass model. The glassy behavior in sintered granular high- T_c $\text{YBa}_2\text{Cu}_3\text{O}_{7-\delta}$ seems to be due to disorder in the intergranular Josephson couplings.

ACKNOWLEDGMENTS

The authors would like to thank Dr. D. H. Kim in Korea Institute of Science and Technology for his stimulating discussions on this work. This work has been supported in part by the non-directed research fund, Korean Research Foundation and in part by Korean Institute of Science and Technology under Grant No. 93-HN-157. One of the authors (S.S.C.) acknowledges support from Korean Ministry of Science and Technology under Grant No. N10310.

*Present address: Department of Physics, Ewha Womans University, Seoul, Korea.

†Present address: Department of Physics, Kon Kuk University, Seoul 133-701, Korea.

¹K. A. Müller, M. Takashige, and J. G. Bednorz, *Phys. Rev. Lett.* **48**, 1143 (1987).

²Y. Yeshurun and A. P. Malozemoff, *Phys. Rev. Lett.* **60**, 2202 (1988).

³See, e.g., A. P. Malozemoff, in *Physical Properties of High Temperature Superconductors I*, edited by D. M. Ginzburg (World Scientific, Singapore, 1989), p. 71.

⁴T. K. Worthington, W. J. Gallagher, and T. Dinger, *Phys. Rev. Lett.* **59**, 1160 (1987).

⁵A. P. Malozemoff, T. K. Worthington, Y. Yeshurun, F. Holtzberg, and P. H. Kes, *Phys. Rev. B* **38**, 7203 (1988).

⁶P. L. Gammel, *J. Appl. Phys.* **67**, 4676 (1990).

⁷T. T. M. Palstra, B. Batlogg, R. B. van Dover, L. F. Schneemeyer, and J. V. Waszczak, *Phys. Rev. B* **41**, 6621 (1990).

⁸G. Deutscher and K. A. Müller, *Phys. Rev. Lett.* **59**, 1745 (1987).

⁹K. W. Blazey, K. A. Müller, J. G. Bednorz, W. Berlinger, G. Amoretti, E. Buluggiu, A. Vera, and C. Maticotta, *Phys. Rev. B* **36**, 7241 (1987).

¹⁰P. W. Anderson, *Phys. Rev. Lett.* **9**, 309 (1962).

¹¹Y. B. Kim, C. F. Hempstead, and A. R. Strnad, *Phys. Rev. Lett.* **12**, 145 (1964).

¹²M. Tinkham, *Phys. Rev. Lett.* **13**, 804 (1964).

¹³M. Tinkham, *Phys. Rev. Lett.* **61**, 1658 (1988).

¹⁴M. Tinkham and C. J. Lobb, *Solid State Physics: Advances in Research and Applications*, edited by H. Ehrenreich and D. Turnbull (Academic, New York, 1989), Vol. 42, p. 91.

¹⁵I. Morgenstern, in *Earlier and Recent Aspects of Superconductivity*, edited by J. G. Bednorz and K. A. Müller (Springer-Verlag, Berlin, 1990), p. 240; see also Ref. 3.

¹⁶L. Ji, M. S. Rzchowski, and M. Tinkham, *Phys. Rev. B* **42**, 4838 (1990).

¹⁷F. Perez, X. Obradors, and J. Fontcuberta, *Physica C* **185-189**,

- 1843 (1991).
- ¹⁸X.-D. Chen, S. Y. Lee, J. P. Golben, S.-I. Lee, R. D. McMichael, Y. Song, T. W. Noh, and J. R. Gaines, *Rev. Sci. Instrum.* **58**, 1565 (1987).
- ¹⁹M. Nikolo and R. B. Goldfarb, *Phys. Rev. B* **39**, 6615 (1989).
- ²⁰K.-H. Müller, *Physica C* **159**, 717 (1989).
- ²¹J. Z. Sun, M. J. Scharen, L. C. Bourne, and J. R. Schrieffer, *Phys. Rev. B* **44**, 5275 (1991).
- ²²D. Stroud and C. Ebner, *Physica C* **153-155**, 51 (1988).
- ²³J. R. Clem, *Physica C* **153-155**, 63 (1988).
- ²⁴V. A. Khlus and A. V. Dyomin, in *Superconductivity and Its Applications*, edited by Yi-Han Kao, Philip Coppens, and Hoi-Sing Kwok, AIP Conf. Proc. No. 219 (AIP, New York, 1991), p. 241.
- ²⁵J. R. Clem, in *Magnetic Susceptibility of Superconductors and Other Spin Systems*, edited by R. A. Hein, T. Francavilla, and D. Liebenburg (Plenum, New York, 1992), p. 177.
- ²⁶V. B. Geshkenbein, V. M. Vinokur, and R. Fehrenbacher, *Phys. Rev. B* **43**, 3748 (1991).
- ²⁷D. X. Chen, R. B. Goldfarb, J. Nogues, and K. V. Rao, *J. Appl. Phys.* **63**, 980 (1988).
- ²⁸S. L. Shinde, J. Morril, D. Goland, D. A. Chance, and T. McGuire, *Phys. Rev. B* **41**, 8838 (1990).
- ²⁹C. Ebner and D. Stroud, *Phys. Rev. B* **31**, 165 (1985).
- ³⁰J. R. L. de Almeida and D. J. Thouless, *J. Phys. A* **11**, 983 (1978).
- ³¹D. C. Cronmeyer and F. Holtzberg, in *Physical Properties of High Temperature Superconductors* (Ref. 3), p. 78.
- ³²G. Deutscher, in *Earlier and Recent Aspects of Superconductivity* (Ref. 15), p. 174; see also Ref. 3.
- ³³J. F. Kwak, E. L. Venturini, P. J. Nigrey, and D. S. Ginley, *Phys. Rev. B* **37**, 9749 (1988).
- ³⁴W. M. Tiernan and R. B. Hallock, *Phys. Rev. B* **46**, 3688 (1992).
- ³⁵X. C. Jin, Y. Y. Xue, Z. J. Huang, J. Bechtold, P. H. Hor, and C. W. Chu, *Phys. Rev. B* **47**, 6082 (1993).

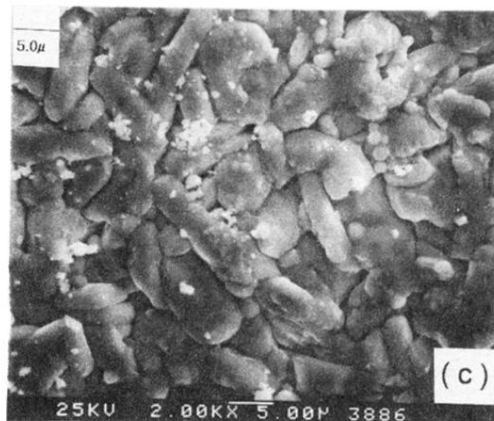
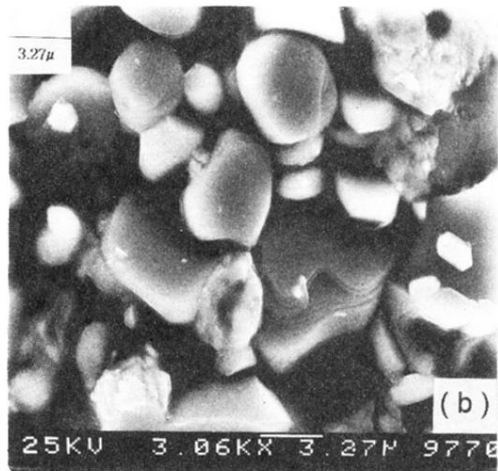
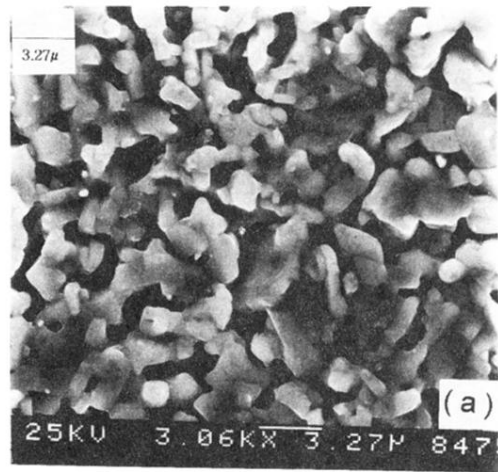


FIG. 1. (a) An SEM picture of sample *A1* (bulk *A*). Most grains are about $1\text{--}2\ \mu\text{m}$ in size. (b) An SEM picture of sample *B* (bulk *B*). Most grains appear $3\text{--}6\ \mu\text{m}$ in size, larger than the average grain size in sample *A1* (bulk *A*). (c) An SEM picture of sample *C* (bulk *C*). Most grains appear $3\text{--}6\ \mu\text{m}$ in size, comparable to the grain size in sample *B* (bulk *B*) and larger than the average grain size in sample *A1* (bulk *A*).